International Journal of Heat and Mass Transfer 52 (2009) 9–16

Contents lists available at ScienceDirect

International Journal of Heat and Mass Transfer

journal homepage: www.elsevier.com/locate/ijhmt

Modelling He I–He II phase transformation in long channels containing superconductors

M. Sitko, B. Skoczeń *,[1]

Faculty of Mechanical Engineering, Centre for Particle Accelerators Design, Cracow University of Technology, Jana Pawła II 37 Ave., 31-864 Cracow, Poland

ARTICLE INFO

Article history:
Received 29 May 2008
Available online 22 July 2008

Keywords:
Superfluid helium
Phase transformation
Heat transport
Temperature profiles

ABSTRACT

The problem of heat transport during sub-cooling below λ point in long, narrow channels containing superconductors immersed in liquid helium is discussed. In order to describe the propagation of phase transformation front the travelling plane wave description with suitable change of variables has been adopted. Nonlinear temperature profile corresponding to the conductivity function in He II has been assumed. The heat diffusion equation is solved in the volume of He I with the assumption that the main contribution to the specific heat is due to helium and the main contribution to longitudinal conduction is due to superconductor. For one dimensional problem with the temperatures clamped at both extremities of the channel the closed form analytical solutions for temperature profile are obtained. Channels with discontinuity in diameter are also analysed. Experimental validation of the model is based on 54 m long superconducting lines applied in the Large Hadron Collider (LHC).

1. Introduction: cable-in-conduit problem

The problem of heat transport in long, narrow channels containing superconductors and filled with superfluid helium has recently gained a lot of interest in view of applications in modern scientific instruments. As the superconducting particle accelerators cooled by means of liquid helium reached the temperatures below lambda point [1], the rate of the He I–He II phase transformation process becomes of primary importance both for standard cool-down and for quench recovery.

Modelling He I–He II phase transition can be carried out either in the framework of condensation mechanism characteristic of ideal Bose–Einstein gas or in the framework of macroscopic two-fluid system proposed by Tisza [2]. In the light of Tisza theory of liquid helium, He II in the temperature range above 1 K and below T_λ forms a mixture of normal component and a superfluid component. The macroscopic thermo-hydrodynamic properties of such two-fluid system have been shown to stay in good agreement with experiment. The thermodynamics of two-fluid model of He II has been further developed by Gorter [3] who has shown that the model requires specific expressions for Gibbs potential of the liquid. Thanks to this macroscopic two-fluid framework the mass and heat transport in He II can be quantitatively described by means of equations similar to classical liquids.

In the present paper the so-called superconducting lines in the form of long narrow channels containing superconductors and filled initially with liquid helium at a temperature above T_λ are analysed. Often, such superconducting lines are housed in the continuous cryostat, parallel to main cold mass (sequence of superconducting magnets) and are connected to the source of He II at one extremity [1]. The process of He I–He II phase transition in such channels takes the form of propagation of the so-called lambda front (initiated close to the source of He II), which is a substantial simplification of the real heat transport of quantum nature in turbulent helium. Nevertheless, such simplified 1D model allows already a quantitative analysis of sub-cooling time of the channel. The process of cool-down below T_λ in long narrow configuration may be substantially delayed with respect to main cold-mass (magnets), due to much smaller active cross-section of He II available usually at one extremity of the channel. Therefore analysis of the subcooling rate as well as of the temperature profile in the channel turns out fundamental for safe powering of superconductors in the line.

The rate of He I–He II phase transformation in long narrow channels has been investigated by Dresner [4] with the aim of obtaining the closed form solutions. The model is based on concentric configuration of copper cable located in the axis of long narrow channel and filled with He I and He II, separated by lambda front propagating at a variable rate. A simplified assumption of linear temperature profile in He II has been made. Moreover, the author assumed that the main contribution to the specific heat is due to helium and the main contribution to longitudinal conduction is due to copper. Also, the heat transport in radial direction has been

* Corresponding author. Tel.: +48 12 628 33 84.
E-mail address: Blazej.Skoczen@pk.edu.pl (B. Skoczeń).
[1] Former CERN Staff member.

0017-9310/$ - see front matter © 2008 Elsevier Ltd. All rights reserved.
doi:10.1016/j.ijheatmasstransfer.2008.06.009

neglected. Thus, the model has been reduced to its one-dimensional form. With the assumption of Gorter-Mellink equation for superfluid helium:

$$\dot{q} = \left[f(T) \frac{\mathrm{d}T}{\mathrm{d}x} \right]^{\frac{1}{3}} \tag{1}$$

where $f(T)$ denotes the heat conductivity function, the following solution for the lambda front propagation rate has been derived:

$$v = \frac{[f(T)\Delta T_{\mathrm{He\,II}}]^{\frac{1}{3}}}{C_{\mathrm{He\,I}} \Delta T_{\mathrm{He\,I}} x_{\lambda}^{\frac{1}{3}}} \tag{2}$$

where $C_{\mathrm{He\,I}}$ denotes the specific heat, $\Delta T_{\mathrm{He\,I}}$, $\Delta T_{\mathrm{He\,II}}$ denote the temperature increments in He I and in He II, respectively, and x_{λ} is the current distance of lambda front from the beginning of the channel. It is worth pointing out that the temperature has been fixed at both extremities of the channel (clamped temperature problem). The solution—even if simplified—indicates that the propagation rate is inversely proportional to the current position of lambda front to the power of 1/3. This means that in the case of infinite channel the phase transformation rate tends to zero. Similar model has been applied by Kowalczyk et al. [5] to the process of subcooling of a superconducting line, used to power the corrector magnets in the Large Hadron Collider (LHC). Further development of this model backed by some experimental results is due to Capatina et al. [6]. Quite similar problem of temperature profiles due to pulsed-source problem has been investigated by Lottin and Van Sciver [7]. Another model of recovery from burnout has been developed by Seyfert et al. [8]. Much more sophisticated model of heat and mass transport in two-phase He II/vapour has been derived by Van Sciver [9]. Helium flow in the channel has been assumed one-dimensional and stratified. Mass exchange between both phases has been allowed. Temperature profiles and the vapour mass flow rate have been obtained by the author. Numerical simulation of the He II–He I phase transition in the "cable-in-conduit" conductor (CICC) has been performed by Mao et al. [10]. One dimensional heat conduction in the longitudinal direction has been assumed. Initially static He II bath combined with negligible transport of mass during the phase transition has been accounted for. The enthalpy method and the moving grid method have been adopted in order to solve the Stefan problem. A combination of method of lines and forward Euler scheme has been used to solve the ordinary differential equations. The evolution of helium temperature accompanied by the He II–He I phase transition provoked by the AC losses and index heating have been successfully simulated. Also, a trajectory of the He II–He I travelling front has been tracked by means of the moving grid method.

The present paper constitutes further step in the direction of obtaining temperature profiles in long channels sub-cooled below T_{λ} and containing superconductors immersed in liquid helium. In order to describe the propagation of phase transformation front (lambda front) the travelling plane wave description with suitable change of variables has been adopted. Temperature profiles on either side of phase transformation front have been derived. In particular, nonlinear temperature profile in He II corresponding to heat conductivity function has been found. The heat diffusion equation is solved in the volume of He I under the assumption that the main contribution to the specific heat is due to helium and the main contribution to longitudinal conduction is due to superconductor. Since He I–He II phase transition is not characterised by any latent heat (phase transition of the second kind according to the Ehrenfest classification [11]), the condition of equal heat fluxes on both sides of lambda front is satisfied. For one dimensional problem with the temperatures clamped at both extremities of the channel the closed form analytical solutions for temperature profile are obtained. Channels with discontinuity in diameter are also analysed. Experimental validation of the model based on 54 m long superconducting lines, applied in the LHC to power the corrector magnets is included [12,13].

2. Heat transport in narrow channels of constant diameter

Heat transport in a long, narrow channel of constant diameter is illustrated in Fig. 1. The channel is filled with He II and He I in the range of temperatures from T_0 to T_{λ} and from T_{λ} to T_{end}, respectively. It is assumed that lambda front moves along the channel at a speed v. Furthermore, it is assumed that both He I and He II are in quasi-steady state, heat transport in superfluid helium is turbulent (above the critical heat flux $\dot{q}_c$) and there is no radial heat transfer across the wall. Thus, one-dimensional model of heat transfer is considered. The use of 1D model is justified when modelling heat transport in long channels of small diameter when compared to its length.

To describe heat transport in He II, the Gorter–Mellink equation in its 1D version is used:

$$\dot{q}^3 \mathrm{d}x = f(T)\mathrm{d}T \tag{3}$$

where $\dot{q}$ denotes the heat flux, dT is the temperature increment on the length dx and $f(T)$ is the heat conductivity function (Fig. 2).

For a given position x_{λ} of the lambda front in the channel and boundary temperatures T_0 and T_{λ} one obtains due to separation of variables:

$$\int_0^{x_{\lambda}} \dot{q}^3 \mathrm{d}x = \int_{T_0}^{T_{\lambda}} f(T)\mathrm{d}T \tag{4}$$

Assuming that the cross-section of the channel is constant, the above equation can be simplified to the following form:

$$\dot{q}(x_{\lambda}) = \left[\frac{\int_{T_0}^{T_{\lambda}} f(T)\mathrm{d}T}{x_{\lambda}} \right]^{\frac{1}{3}} \tag{5}$$

Here, the assumption of equal heat flux in every superfluid section of the channel has been made [9]. In view of the above equation, it turns out that the value of the heat flux in a tube of constant diameter depends inversely on the cubic root of the lambda front position (Fig. 3):

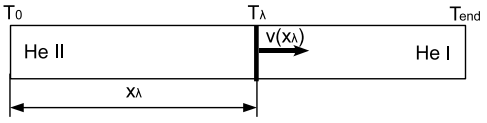

Fig. 1. Tube filled with liquid helium.

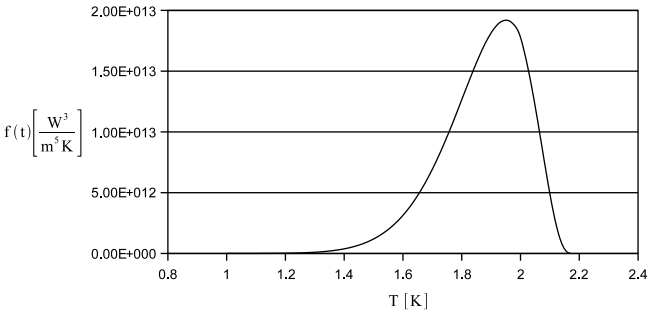

Fig. 2. Superfluid helium heat conductivity function at 1,3 bar [14].

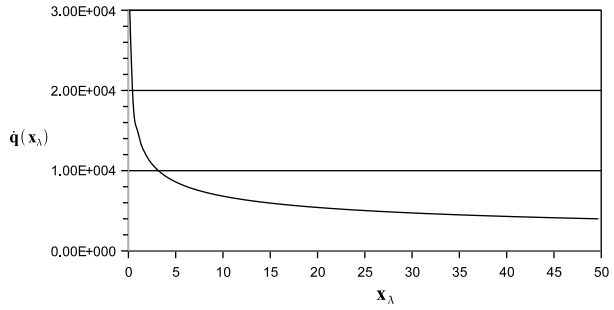

Fig. 3. Heat flux as a function of x_λ in channel of constant diameter.

$$\dot{q}(x_\lambda) = \left(\frac{C}{x_\lambda}\right)^{\frac{1}{3}} = \frac{\widetilde{C}}{\sqrt[3]{x_\lambda}} \tag{6}$$

where C denotes the integrated conductivity function and is a constant value.

If the heat flux is known, the velocity of the lambda front can be determined by using the amount of energy extracted from He I:

$$dQ = m \cdot c_p \cdot \mathrm{d}T \tag{7}$$

Integrating Eq. (7) from T_λ to T_{end} one obtains the amount of heat which is transported from He I to He II in the course of the phase transformation process.

$$\Delta Q = \int_{T_\lambda}^{T_{\mathrm{end}}} m \cdot c_p(T) \cdot \mathrm{d}T \tag{8}$$

The mass of helium can be expressed as volume multiplied by density, so that:

$$\Delta Q = S \cdot \Delta x \int_{T_\lambda}^{T_{\mathrm{end}}} \rho(T) \cdot c_p(T) \cdot \mathrm{d}T \tag{9}$$

The evolution of lambda front is illustrated in Fig. 4. For the time period $\Delta t = t_2 - t_1$ lambda front moves by Δx and the heat is extracted from the volume $S \cdot \Delta x$, where S is the cross-section area of the channel. It is worth pointing out that the motion of the lambda front is strongly justified by the second order phase transition, where both phases cannot coexist in thermodynamic equilibrium.

Transport of energy across the lambda front can be expressed in the following way:

$$\frac{\Delta q}{\Delta t} = \frac{\Delta x}{\Delta t} \int_{T_\lambda}^{T_{\mathrm{end}}} \rho_{\mathrm{He\,I}}(T) \cdot c_{p\mathrm{He\,I}}(T) \cdot \mathrm{d}T \tag{10}$$

where $\Delta q = \frac{\Delta Q}{S}$.

When the time interval is sufficiently small $\Delta t \to \mathrm{d}t$, the heat flux can be approximately calculated as follows:

$$\frac{\mathrm{d}q}{\mathrm{d}t} = \frac{\mathrm{d}x}{\mathrm{d}t} \int_{T_\lambda}^{T_{\mathrm{end}}} \rho_{\mathrm{He\,I}}(T) \cdot c_{p\mathrm{He\,I}}(T) \cdot \mathrm{d}T \tag{11}$$

Here, a simplified assumption of temperature distribution reaching T_{end} over the distance of Δx in He I has been made. Given very steep increase of temperature in He I in the proximity of λ transition, the above assumption is not far from reality.

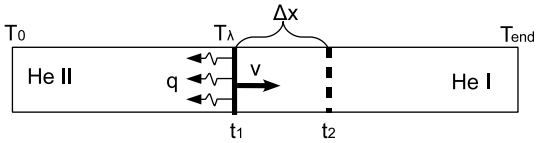

Fig. 4. Lambda front propagation.

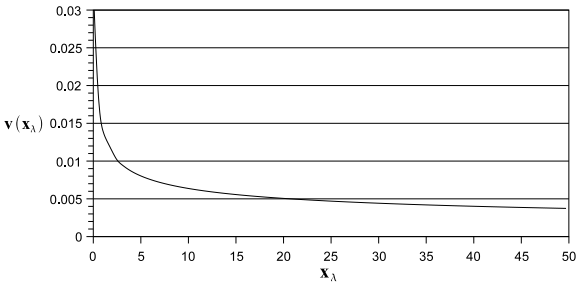

Fig. 5. Velocity of lambda front as a function of its position.

Finally, the following approximate formula for lambda front velocity is obtained.

$$v(x_\lambda) = \frac{\dot{q}(x_\lambda)}{\int_{T_\lambda}^{T_{\mathrm{end}}} \rho_{\mathrm{He\,I}}(T) \cdot c_{p\mathrm{He\,I}}(T) \cdot \mathrm{d}T} \tag{12}$$

As the heat flux transported across the lambda front is inversely proportional to the cubic root of lambda front position (Eq. (6)) and the integral in denominator of Eq. (12) is constant, the front velocity decays in a similar way like the flux (Fig. 5).

Knowing the velocity of lambda front propagation, the time of subcooling can be derived as:

$$t = \int_0^L \frac{\mathrm{d}x}{v(x_\lambda)} \tag{13}$$

where L denotes the length of the channel.

3. Temperature profiles on either side of phase transformation front

3.1. Temperature profile in He II

In order to determine temperature profile in He II, a channel of constant diameter and length L, cooled at one end by infinite reservoir of helium bath of constant temperature $T_0 < T_\lambda$ is considered (Fig. 4). The relationship between temperature and distance can be derived from Gorter–Mellink law (3), assuming steady-state heat transport and constant heat flux along the channel [9]. This assumption is true for lambda front located already far enough from the beginning of the channel.

$$x(T) = \frac{\int_{T_0}^{T} f(\eta)\mathrm{d}\eta}{\dot{q}^3_{\mathrm{He\,II}}} \tag{14}$$

An example of temperature profile in the channel filled with He II with boundary temperatures $T_0 = 1.9K$ and $T_\lambda = 2.17K$ is shown in Fig. 6.

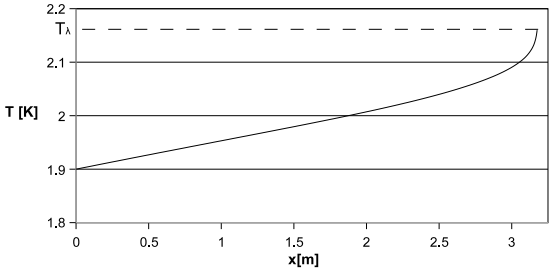

Fig. 6. Temperature profile in superfluid helium (below T_λ).

3.2. Temperature profile in He I

The temperature profile in He I is obtained for concentric configuration of superconductor located in the middle of long, narrow channel filled with liquid helium, as illustrated in Fig. 7. Heat transfer in He I and in the cable can be written in the form of second order differential equation:

$$[(\rho c_p A)_{\mathrm{He\,I}} + (\rho c_p A)_{\mathrm{Cu}}]\frac{\partial T}{\partial t} = [(kA)_{\mathrm{He\,I}} + (kA)_{\mathrm{Cu}}]\frac{\partial^2 T}{\partial x^2} \tag{15}$$

Here, perfect heat transport between superconductor and helium in the radial direction has been assumed. The specific heat of copper is small when compared to helium as well as the conductivity of helium is insignificant when compared to copper. Omitting small terms, the Eq. (15) can be simplified to the following form:

$$\frac{\partial T}{\partial t} = D\frac{\partial^2 T}{\partial x^2} \tag{16}$$

where $D = \frac{(kA)_{\mathrm{Cu}}}{(\rho c_p A)_{\mathrm{He\,I}}}$ is a combined thermal diffusivity and—for the sake of simplicity—is assumed to be constant in the range of temperatures from T_λ to T_{end}.

As the problem is spacio-temporary, a plane wave approach based on the suitable change of variables is applied. The change of variables takes the form known in the problem of ablation: $\xi = x - vt$. New variable makes it easier to analyse the heat transport problem assuming that the beginning of coordinate system moves together with lambda front. Thus, Eq. (16) transforms into:

$$\frac{\partial T}{\partial t} = D\frac{\partial^2 T}{\partial \xi^2} - v(t)\frac{\partial T}{\partial \xi} \tag{17}$$

The heat diffusion Eq. (17) can be solved by applying the method of separation of variables. The general solution is then expressed as a product of a function of ξ and a function of t with additional constant value T_{end} which denotes the temperature at the end of the channel:

$$T(\xi, t) = \Phi(t)\Psi(\xi) + T_{\mathrm{end}} \tag{18}$$

Differentiating the functions $\Phi(t)$ and $\Psi(\xi)$ and inserting them into Eq. (17) one obtains:

$$\Psi\frac{\partial \Phi}{\partial t} = D\Phi\frac{\partial^2 \Psi}{\partial \xi^2} - v(t)\Phi\frac{\partial \Psi}{\partial \xi} \tag{19}$$

In order to simplify the solution, the assumption of constant velocity v of the lambda front is made. This assumption is justified when lambda front is already far enough from the beginning of the channel (Fig. 5, flat part of the curve $v(x)$). The final form of the heat diffusion equation can be written as follows:

$$\frac{1}{D\Phi}\frac{\partial \Phi}{\partial t} = \frac{1}{\Psi}\frac{\partial^2 \Psi}{\partial \xi^2} - \frac{v}{D\Psi}\frac{\partial \Psi}{\partial \xi} \tag{20}$$

Since the left hand side of Eq. (20) is function of t alone and the right hand side is function of ξ alone, the only possible solution implies that they are both equal to a separation constant k^2. Thus:

$$\frac{1}{D\Phi}\frac{\partial \Phi}{\partial t} = -k^2 \tag{21}$$

$$\frac{1}{\Psi}\frac{\partial^2 \Psi}{\partial \xi^2} - \frac{v}{D\Psi}\frac{\partial \Psi}{\partial \xi} = -k^2 \tag{22}$$

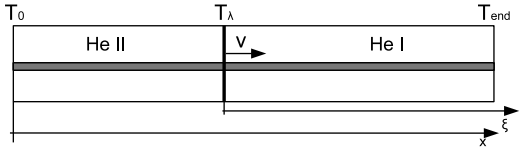

Fig. 7. Cable-in-conduit problem.

Eq. (21) is in fact the first-order ordinary differential equation. It can be solved by integrating both sides of the equation.

$$\frac{\mathrm{d}\Phi}{\Phi} = -k^2 D\,\mathrm{d}t \tag{23}$$

The general solution of Eq. (23) reads:

$$\Phi(t) = C_1 \mathrm{e}^{-Dk^2 t} \tag{24}$$

Eq. (22) is a linear homogeneous second order differential equation:

$$\frac{\partial^2 \Psi}{\partial \xi^2} + \frac{v}{D}\frac{\partial \Psi}{\partial \xi} + k^2\Psi = 0 \tag{25}$$

The solution of (25) can be assumed in the form of exponential function:

$$\Psi = \mathrm{e}^{\lambda\xi} \tag{26}$$

Inserting the solution (26) into Eq. (25) one obtains:

$$\mathrm{e}^{\lambda\xi}\left(\lambda^2 + \frac{v}{D}\lambda + k^2\right) = 0 \tag{27}$$

A non-trivial, real solution of Eq. (27) exists if $\Delta = \left(\frac{v}{D}\right)^2 - 4k^2 \geqslant 0$. Then, the general solution of Eq. (22) takes the form:

$$\Psi(\xi) = C_2\mathrm{e}^{\lambda_1\xi} + C_3\mathrm{e}^{\lambda_2\xi} \tag{28}$$

where:

$$\lambda_1 = \frac{-v + \sqrt{v^2 - 4D^2k^2}}{2D} \tag{29}$$

$$\lambda_2 = \frac{-v - \sqrt{v^2 - 4D^2k^2}}{2D} \tag{30}$$

Finally, referring back to Eq. (18) one obtains the general solution:

$$T(\xi, t) = \mathrm{e}^{-Dk^2 t}\cdot\left(A\mathrm{e}^{\lambda_1\xi} + B\mathrm{e}^{\lambda_2\xi}\right) + T_{\mathrm{end}} \tag{31}$$

where: $A = C_1 \cdot C_2$ and $B = C_1 \cdot C_3$.

The values of A and B can be calculated by applying the following boundary conditions:

$$T(\xi \to 0) = T_\lambda \tag{32}$$

$$\frac{\partial T}{\partial \xi}(\xi \to 0) = \frac{A_{\mathrm{He\,II}}}{A_{\mathrm{Cu}}k_{\mathrm{Cu}}}\dot{q}_\lambda \tag{33}$$

Finally, one obtains:

$$A = \frac{[(T_{\mathrm{end}} - T_\lambda)\lambda_2 + \widetilde{D}\dot{q}_\lambda]\mathrm{e}^{Dk^2t}}{\lambda_1 - \lambda_2} \tag{34}$$

$$B = [(T_{\mathrm{end}} - T_\lambda) - \frac{(T_{\mathrm{end}} - T_\lambda)\lambda_2 + \widetilde{D}\dot{q}_\lambda}{\lambda_1 - \lambda_2}]\mathrm{e}^{Dk^2t} \tag{35}$$

where $\widetilde{D} = \frac{A_{\mathrm{He\,II}}}{A_{\mathrm{Cu}}k_{\mathrm{Cu}}}$. By inserting A and B into Eq. (31), the expression for temperature profile in He I region is obtained:

$$T(\xi, t) = T_{\mathrm{end}} + \frac{T_{\mathrm{end}} - T_\lambda}{\lambda_1 - \lambda_2}(\lambda_2\mathrm{e}^{\lambda_1\xi} - \lambda_1\mathrm{e}^{\lambda_2\xi}) + \frac{\widetilde{D}\dot{q}_\lambda}{\lambda_1 - \lambda_2}(\mathrm{e}^{\lambda_1\xi} - \mathrm{e}^{\lambda_2\xi}) \tag{36}$$

The temperature profile in the proximity of lambda transition is illustrated in Fig. 8.

4. Channels containing bifurcation or discontinuity in diameter

In order to model a channel with one discontinuity in diameter (Fig. 9) the assumption of energy conservation has to be made. Thus, the heat flux multiplied by the area of cross-section is assumed to be constant along the channel. According to the energy conservation law:

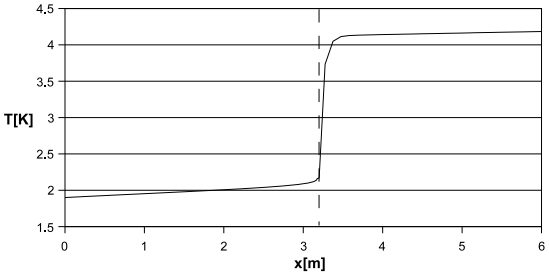

Fig. 8. Temperature profile in the channel containing copper cable.

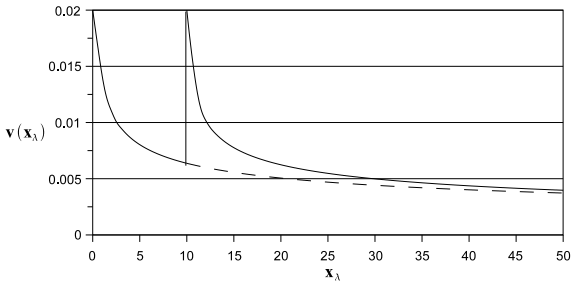

Fig. 10. Velocity of lambda front in the channel with discontinuity in diameter.

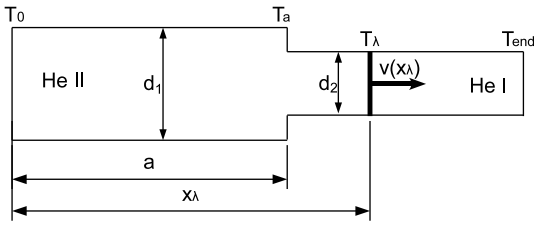

Fig. 9. Tube filled with liquid helium with discontinuity of diameter.

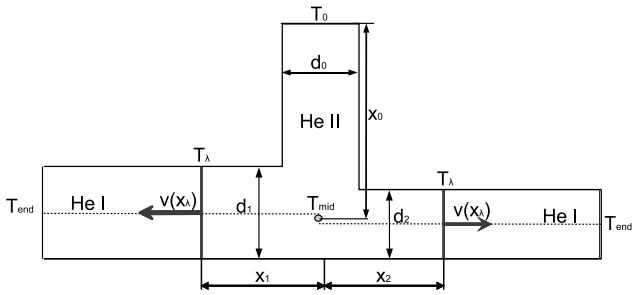

Fig. 11. Channel with bifurcation filled with liquid helium.

$$\dot{q}_1 S_1 = \dot{q}_2 S_2 \tag{37}$$

Now, Eq. (1) can be applied to both parts of the channel shown in Fig. 9:

$$\dot{q}_1(x_\lambda) = \left[\frac{\int_{T_0}^{T_a} f(T)\mathrm{d}T}{a}\right]^{\frac{1}{3}} \quad \text{and} \quad \dot{q}_2(x_\lambda) = \left[\frac{\int_{T_a}^{T_\lambda} f(T)\mathrm{d}T}{x_\lambda - a}\right]^{\frac{1}{3}} \tag{38}$$

where a is the length of the left hand portion of the channel with respect to the change of the diameter and T_a denotes the temperature at the cross-sectional discontinuity.

Transforming Eqs. (37) and (38), one obtains the equation representing heat flux in the channel beyond the discontinuity:

$$\dot{q}_2(x_\lambda) = \frac{1}{S_2}\left[\frac{\int_{T_0}^{T_\lambda} f(T)\mathrm{d}T}{\frac{a}{S_1^3} - \frac{x_\lambda - a}{S_2^3}}\right]^{\frac{1}{3}} \tag{39}$$

The above equation can be generalised [15] to the case with multiple changes of diameter along the channel as follows:

$$\dot{q}_1 S_1 = \ldots = \dot{q}_N S_N \tag{40}$$

$$\dot{q}_N(x_\lambda) = \frac{1}{S_N}\left[\frac{\int_{T_0}^{T_\lambda} f(T)\mathrm{d}T}{\sum_{i=1}^{N-1}\frac{l_i}{S_i^3} - \frac{x_\lambda - \sum_{i=1}^{N-1} l_i}{S_N^3}}\right]^{\frac{1}{3}} \tag{41}$$

where N is the number of discontinuities and l_i is the length of sections between discontinuities.

The velocity of lambda front is calculated similarly as in the model of constant diameter according to Eq. (12). However, sudden increase of velocity is observed when lambda front passes the point of diameter change (continuous line in Fig. 10).

It is worth pointing out that the change of the section from wider to narrower increases the velocity, while in the opposite situation the velocity decreases.

The bifurcation corresponds to "T" shaped connection (Fig. 11). The solution is trivial when the diameters d_1 and d_2 are equal. It becomes more complex when the diameters are different.

Once again, according to energy conservation law one obtains:

$$\dot{q}_0 S_0 = \dot{q}_1 S_1 + \dot{q}_2 S_2 \tag{42}$$

where the heat fluxes are expressed by:

$$\dot{q}_0 = \left[\frac{\int_{T_0}^{T_{\mathrm{mid}}} f(T)\mathrm{d}T}{x_0}\right]^{\frac{1}{3}} \tag{43}$$

$$\dot{q}_1 = \left[\frac{\int_{T_{\mathrm{mid}}}^{T_\lambda} f(T)\mathrm{d}T}{x_1}\right]^{\frac{1}{3}}, \quad \dot{q}_2 = \left[\frac{\int_{T_{\mathrm{mid}}}^{T_\lambda} f(T)\mathrm{d}T}{x_2}\right]^{\frac{1}{3}} \tag{44}$$

Modifying the Eqs. (42)–(44) one obtains:

$$\dot{q}_1(x_\lambda) = \dot{q}_2(x_\lambda) = \frac{1}{S_1 + S_2}\left[\frac{\int_{T_0}^{T_\lambda} f(T)\mathrm{d}T}{\frac{x_0}{S_0^3} + \frac{x_\lambda - x_0}{(S_1+S_2)^3}}\right]^{\frac{1}{3}} \tag{45}$$

Because $\dot{q}_1(x_\lambda)$ and $\dot{q}_2(x_\lambda)$ are equal, the position of lambda fronts on both sides of the bifurcation are the same.

5. Experimental validation

To verify the analytical model of heat transport and He I–He II phase transformation rate the measurements have been carried out by means of an experimental setup. The setup was built as a full scale model of superconducting line used to power the corrector magnets in the LHC [12,13]. The superconducting line constituted a 50 mm ID tube, composed of 2 segments, each 54 m long, attached to the superconducting magnets and cooled at one extremity via a direct link to the bulk of He II. The line is illustrated in Fig. 12.

The process of subcooling (cooling from 4.5 to 1.9 K) the channel containing superconductors was computed by using the equations suitable for multiple changes of diameter. The parameters used in the modelling were lengths of channel portions and the cross-section areas.

In the first part of experiment, the superconducting line was connected to the magnets by inlet channel. The magnets formed a suitable large source of bulk He II. At the opposite extremity of the line a polyethylene insert was installed, which considerably reduced the helium cross-section area. Lambda front travelled from inlet channel along the superconducting line.

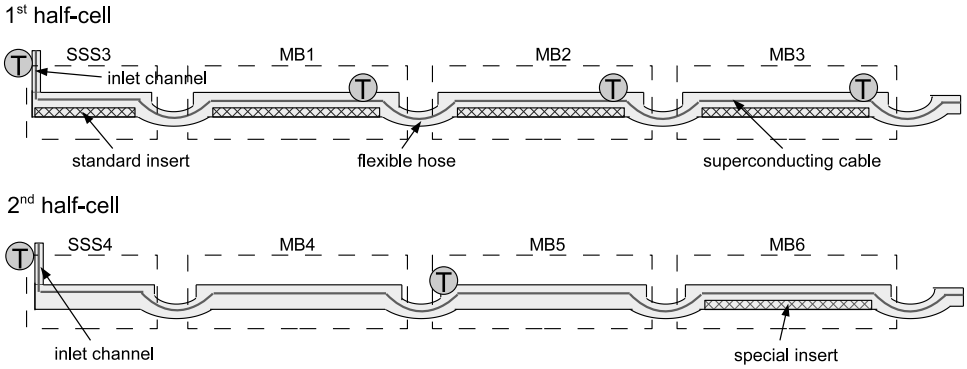

Fig. 12. Superconducting line configuration in the first part of the experiment.

A comparison of calculated and measured subcooling times for the superconducting line during first part of the experiment is shown in Table 1. The possible reason of discrepancy between measurements and calculations may be related to the lack of temperature sensor at the extremity of the 2nd half-cell. The measured values were obtained by extrapolation based on the mean velocity of lambda front in the magnets.

In lambda second part of experiment (Fig. 13) two additional channels connecting superconducting line with magnets were installed in order to increase the inlet helium cross-section. The insert was removed and the superconducting line had constant cross-section area apart from the inlet channels. In addition, a copper barrier extracting heat from the line to the magnets was installed at the extremity of the experimental cell to accelerate the subcooling process. Thus, the lambda front was initiated not only via the inlet channels but also via the copper barrier.

Table 1
Superconducting line experiment – comparison of measurements and computations

Time of subcooling	Measurements [h]	Computations [h]
Part I		
1st half cell	3.1	3.5
2nd half cell	5.5	4.3
Part II		
1st half cell	1.9	3.1
2nd half cell		
1st front	3.7	3.4
2nd front	11.5	10.9
1st and 2nd front	2.2	2.4

The model of the superconducting line subcooled by two lambda fronts is shown in Fig. 14.

The comparison of measured and computed subcooling times for superconducting line during the second part of experiment is shown in Table 1. Three scenarios were considered: lambda front produced by inlet channels (1st lambda front), lambda front produced by the copper barrier (2nd lambda front), simultaneous subcooling by both lambda fronts.

The possible reason of discrepancy in the results, just like in the first part of experiment, may be the lack of suitable temperature sensor at the extremity of the line.

The process of subcooling of superconducting line after quench (resistive transition in magnets) is shown in Fig. 15.

Here, a suitable number of thermometers has been installed. Travelling lambda front can be easily observed in the window shown in Fig. 15 (temperature drops).

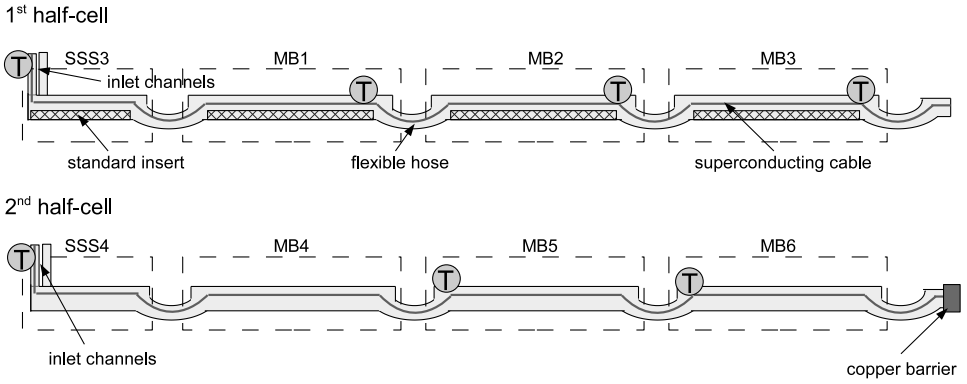

Fig. 13. Superconducting line configuration in the second part of the experiment.

Fig. 14. Model of superconducting line in the second part of the experiment.

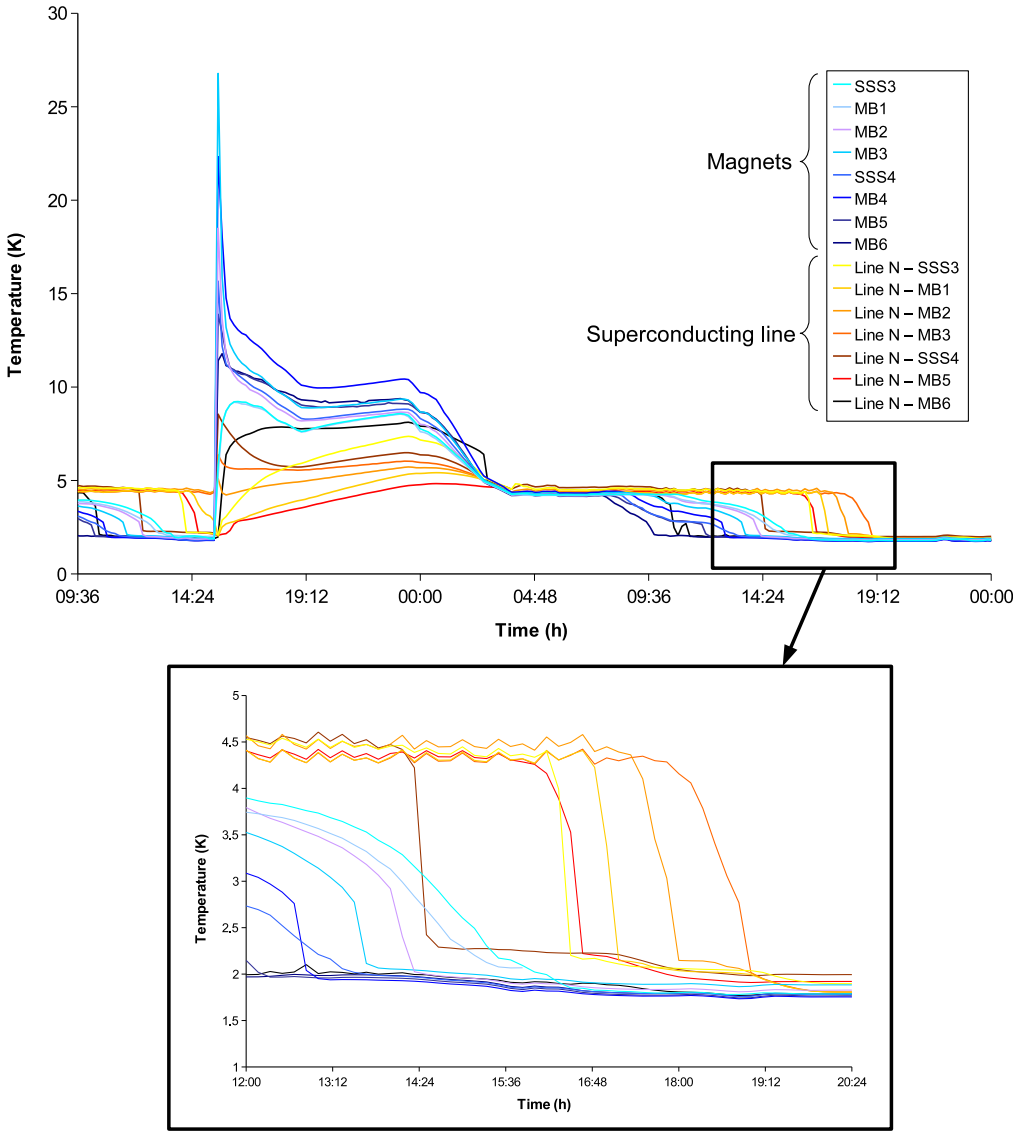

Fig. 15. Temperature profiles during quench recovery in the superconducting line.

6. Application in superconducting particle accelerators

The current model of He I–He II travelling phase transition front has been derived in view of multiple applications in the process of subcooling modern particle accelerators equipped with superconducting magnets. Apart from main magnetic components (dipoles and quadrupoles) these rather complicated machines integrate a sophisticated array of correctors (higher order multipoles) that are often powered via specific auxiliary bus-bar channels (Fig. 16), located next to the main cold mass in the continuous cryostat. Such layout of cryogenic components yields a need to optimise the subcooling process in view of fast cool-down from room temperature to below T_λ and in view of fast quench recovery after resistive transition in a portion of the accelerator. Such approach has been applied in the LHC in order to minimize time of subcooling of the superconducting line, both in the main arc and in the arc extremities (dispersion suppressors). In the process of parametric optimisation of topology of the superconducting line the cross-section of main channel and the cross-section of a periodic link to the source of He II (main magnets) were taken into account. For many reasons, related mainly to space constraints, these cross-sections were limited to the values not necessarily convenient from the thermodynamic point of view. In addition, the available free cross-section of He II in the main channel was mostly

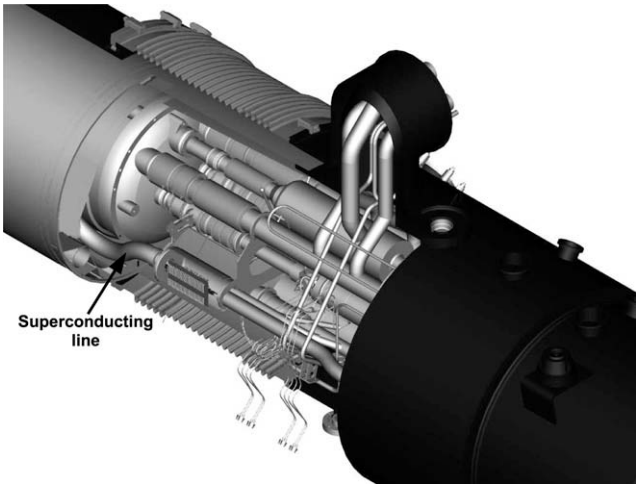

Fig. 16. Superconducting line in front of magnet interconnections (CERN).

limited by the amount of superconductor and polyethylene inserts, variable as a function of the accelerator sector. In order to speed up the process of initial cool-down or the process of quench recovery, special copper membranes playing role of heat exchangers were designed and located in some parts of the machine [16]. Thanks to this solution a number of lambda front sources were created in the superconducting line which considerably reduced its time of subcooling. In all these cases the model derived in the present paper—even if simplified—turned out particularly useful. In most of the cases the mathematically predicted additional time for subcooling the superconducting line did not exceed some 2 h, when compared to main cold mass (dipole and quadrupole magnets). The authors strongly believe that the current model constitutes a useful analytical tool for fast design process of narrow cryogenic channels containing superconductors needed to power specific accelerator systems.

7. Conclusions

Heat transport in long, narrow channels containing superconductors and filled with liquid helium has been investigated by means of analytical approach. It is worth pointing out, that even 1D problem of heat diffusion across lambda transition (front) moving along a narrow channel is rather complicated from the point of view of mathematical description. In order to obtain closed form solutions for the heat flux, lambda front propagation rate and the temperature profile in the channel a number of simplifications has to be made. As the solution of the above mentioned problem is based on the travelling plane wave description with suitable change of variables, it is possible to reduce the equations to quasi-stationary version. However, in order to simplify the transformation of variables a constant propagation rate for the lambda front has to be assumed. This assumption implies the position of lambda front already far enough from the beginning of the channel. Therefore, the solution presented in the paper corresponds to the flat part of the curve: velocity versus distance. It is worth pointing out, that closed form solution for the temperature profile in He I and in He II has been obtained, which constitutes a step forward when compared to previous publications in this domain [10].

Another observation has been made for channels with discontinuity in diameter. As soon as lambda front reaches a reduction in diameter of the channel, its velocity considerably increases and the process of velocity decay as a function of distance is delayed when compared to the channel of constant diameter. Both in the case of channel of constant diameter and in the case of variable cross-section the velocity decays to zero for the length of channel tending to infinity.

Experimental validation of 1-D model presented in the paper is based on 2×54 m long experimental superconducting line, applied in the LHC to power the corrector magnets [12,13]. The measurements of lambda front propagation rate, carried out during the process of subcooling the channel containing superconductors, converged reasonably well with the analysis carried out by using the model. This is certainly a good indication of validity of the model.

Finally, it is worth pointing out that the model is attractive and useful in the design of cryogenic systems containing He II and subjected to variations of temperature related to temporary heat production sources like superconducting coils. After resistive transition (quench) the system has to be subcooled back to below T_λ and time of this operation has to be minimised. The model provides an efficient tool for the so-called "quench recovery" optimisation process.

Acknowledgement

The authors express gratitude to Dr. Alain Poncet (CERN) for many valuable suggestions and discussions when developing the model presented in the paper. Grant of Polish Ministry of Science and Higher Education: PB 4T07A 027 30 is gratefully acknowledged.

References

[1] P. Lebrun, Cryogenics for the Large Hadron Collider, IEEE Trans. Appl. Superconductivity 10 (2000) 1500–1506.
[2] L. Tisza, The theory of liquid helium, Phys. Rev. 72 (1947) 838–854.
[3] C.J. Gorter, On the thermodynamics of the two fluid model of helium II, Physica 15 (1949) 523–531.
[4] L. Dresner, Transient heat transfer in superfluid helium – Part II, Adv. Cryogenic Eng. 29 (1984) 323–333.
[5] P. Kowalczyk, A. Poncet, P. Sacre, B. Skoczeń, Thermal performance of the LHC external auxiliary bus-bar tube: mathematical modelling, in: Proceedings of 17th International Cryogenic Engineering Conference (ICEC 17) Bournemouth, UK, 1998.
[6] O. Capatina, A. Poncet, B. Skoczén, Lambda front propagation in the superfluid helium contained in the external auxiliary bus-bar line of the LHC, in: International Cryogenic Materials Conference CEC-ICMC 2003, Alaska, USA, AIP Conf. Proc. 710, 2004, pp. 1068–1078.
[7] J.C. Lottin, S.W. Van Sciver, Heat transport mechanisms in a 2.3-meter-long cooling loop containing He II, in: Proceedings of the 9th International Cryogenic Engineering Conference, Kobe, Japan, 1982.
[8] P. Seyfert, J. Lafferranderie, G. Claudet, Time-dependent heat transport in subcooled superfluid helium, Cryogenics 22 (1982) 401–408.
[9] S.W. Van Sciver, Helium Cryogenics, Plenum Press, 1986.
[10] S. Mao, C.A. Luongo, D.A. Kopriva, Numerical simulation of the He II/He I phase transition in superconducting magnets, Int. J. Heat Mass Trans. 49 (2006) 4786–4794.
[11] G. Jaeger, The Ehrenfest classification of phase transitions: introduction and evolution, Arch. History Exact Sci. 53 (1998) 51–81.
[12] A. Bezaguet et al., The superfluid helium cryogenic system for the LHC test string: design construction and first operation, in: Proceedings of Cryogenic Engineering Conference and International Cryogenic Materials Conference, Columbus – Ohio, USA, 1995.
[13] R. Saban et al., First results and status of the LHC test string 2, in: Proceedings of 8th European Particle Accelerator Conference (EPAC), Paris, France, 2002.
[14] Cryodata,Inc., User's Guide to HEPAK, Version 3.4, 1999.
[15] G. Ottaviani, B. Skoczeń J.R. Thome, Modelisation et analyse du refroidessement des busbars supraconducteurs alimentant les aimants correcteurs du LHC, Diploma Thesis, Ecole Polytechnique Federale de Lausanne/CERN, 2004.
[16] M. Sitko, B. Skoczeń, C. Garion, A. Poncet, F. Seyvet, J.P. Tock, Copper heat exchanger for the external auxiliary bus-bars routing line in the LHC insertion regions, in: Proceedings of 10th European Particle Accelerator Conference (EPAC), Edinburgh, Scotland, 2006.